PREFIRE Data User Guide

Level 1B Radiance (1B-RAD)

Version R01
(20250430)

Erin Hokanson Wagner
Brian Drouin
Tim Michaels
Aronne Merrelli

Table of Contents

1 Introduction

This user guide contains information for the PREFIRE data collections PREFIRE_SAT1_1B-RAD and PREFIRE_SAT2_1B-RAD – version R01 – which are archived by the Atmospheric Science Data Center (ASDC) at the NASA Langley Research Center. These collections contain geolocated and calibrated radiance data from the PREFIRE Thermal Infrared Spectrometer (TIRS) instruments.

1.1 Mission Overview

The Science Mission Directorate (SMD) at NASA Headquarters selected the Polar Radiant Energy in the Far InfraRed Experiment (PREFIRE) as an Earth System Science Pathfinder (ESSP) Earth Venture Instrument (EVI-4) class Mission of Opportunity. Through spectrally resolved observations of radiances spanning the radiatively significant portions of the Mid- and Far-InfraRed (MIR and FIR), PREFIRE addresses two complementary hypotheses:

1. Time-varying errors in both FIR surface emissivity and thermal radiation modulate estimates of energy exchanges between the surface and the atmosphere in the Arctic.
2. These terms are responsible for a large fraction of the spread in projected rates of change for Arctic surface, ocean, and atmosphere characteristics.

These hypotheses are addressed through five related objectives:

O1.1 Quantify snow and ice FIR emissivity spectra and their variability on seasonal scales;
O1.2 Quantify the FIR thermal radiation and its response to seasonal variations in cloud cover / water vapor;
O1.3 Quantify variability in Arctic spectral surface emission and the thermal radiation across the FIR owing to transient cloud and water vapor and sub-daily surface phase-change processes;
O2.2 Quantify thermal emission errors on projected rates of Arctic warming and sea ice loss;
O2.3 Determine the impact of improved surface emissivity on modeled ice sheet dynamic processes on hourly scales.

PREFIRE uses broadband infrared (> 75% of surface emitted thermal radiation) radiance measurements made from the separate orbiting platforms (CubeSats) to address the science objectives. The PREFIRE payloads are two stand-alone instruments built at JPL using heritage from the Mars Climate Sounder and the Moon Mineralogy Mapper. The PREFIRE instruments are thermal infrared imaging spectro-radiometers with more than 50 spectral bands. Each PREFIRE instrument uses ambient temperature thermopile detectors and operates in a pushbroom mode with a point and stare mirror for viewing nadir (Earth), space, and a calibration target. PREFIRE data are calibrated with data from views of the internal calibration target and of space, which are viewed multiple times per orbit.

Soon after launch, the orbit altitude was approximately 531 km for both satellites. However, the PREFIRE CubeSats do not have station-keeping abilities and so their altitudes decrease with time. The current satellite altitude is recorded as *sat_altitude* (*Geometry* data group) in the file data.

The PREFIRE project delivers space-based measurements of radiative fluxes, cloud masks, spectrally variant surface emissivity (ε_λ), and column water vapor (CWV). These are science products with the precision, resolution, and coverage needed to improve our understanding of polar energy balances and Earth-system effects over diurnal and seasonal cycles at scales that capture surface and cloud variability. During its approximately one-year baseline mission, PREFIRE will capture the natural variability in Arctic and Antarctic CWV and surface temperature. PREFIRE reduces uncertainties in the surface and atmospheric components of the polar energy budget.

1.2 Data Overview

PREFIRE Level 1B Radiance data are contained in two collections: PREFIRE_SAT1_1B-RAD and PREFIRE_SAT2_1B-RAD. The data are provided in distinct data collections because the two PREFIRE-TIRS instruments each have different mission timeframes, characterizations, and known issues. Please be sure to read about these differences below.

All Level 1 through Level 3 PREFIRE data products are produced at the PREFIRE Science Data Processing System (SDPS), located at the University of Wisconsin-Madison. Level 0 data are ingested approximately four times per day for each satellite. Level 1B Radiance data are nominally processed on a delay of at least four days from ingest of the Level 0 science data, allowing for data sent from the spacecraft out of chronological order to be incorporated.

1.2.1 Spectral characteristics

Each PREFIRE-TIRS includes a 512-element (64 x 8) Focal Plane Array (FPA) of thermal radiation detectors. This FPA provides 8 spatial “scenes”, each ideally collecting 64 spectral measurements. The 64 spectral elements, labeled as “channels”, consist of a single channel (channel 0) that is illuminated by a direct, undispersed radiation beam, followed by channels 1–63 that collect the dispersed light from the grating. Across these 63 spectral channels, selected channels are physically masked at the wavelength edges of the order sorting filters. There are pairs of masked channels between each of the order sorting filters, and three masked channels at the start of the array. The result is a total of 54 channels designed to be active within each instrument. The full set of 63 channels (and channel 0) is retained during processing, and inactive channels (due to masking) are simply flagged and contain *Fill_Value* within the 1B-RAD product, as these masked channels do not contain usable radiance measurements.

Figure 1-1 shows the spectral sampling of each instrument, which is also summarized in Table 7-1. Each instrument has a distinct "idealized” wavelength sampling for each channel, which is the center wavelength of the grating dispersion at that channel. The mean wavelength for each channel is a weighted average, where the Spectral Response Function (SRF) for each channel supplies the weights.

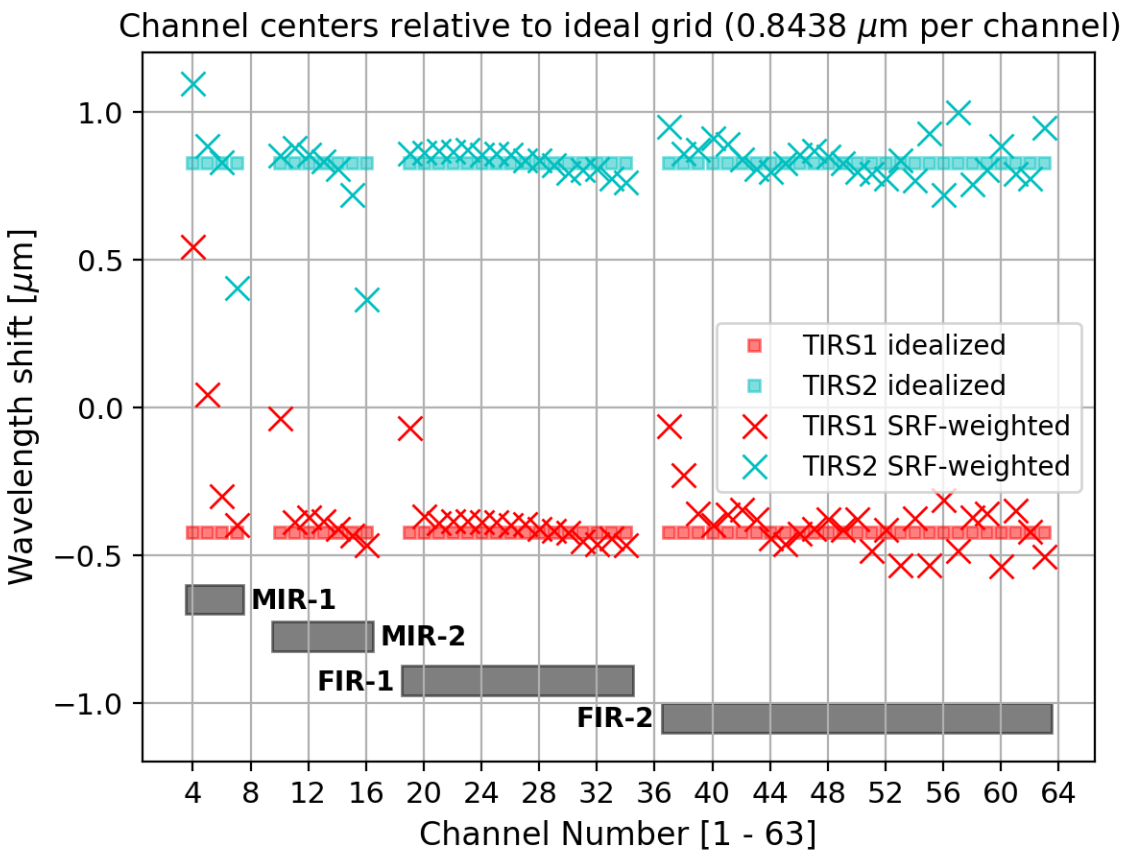

Figure 1-1. The wavelength sampling (in microns per channel) of the two PREFIRE-TIRS instruments is nearly identical, but the two grids are offset by about 1.25 μm. The idealized channel centers are marked with colored squares, and the mean channel wavelengths (weighted by the channel Spectral Response Function) are marked with X. The active channels are split into four spectral bands by order sorting filters within the optical path, labeled here as MIR-1, MIR-2, FIR-1 and FIR-2.

Channel 0 (the undispersed channel) does have a spectrally varying response, as shown in Figure 1-2. The response drops to near zero for short wavelengths (approximately < 3 μm), but the throughput was not characterized at those wavelengths (NIR or visible). Thus, the calibrated flux reported in Channel 0 will contain unquantified amounts of scattered solar radiation at short wavelengths. Any use of Channel 0 data should either focus on scenes at local night times (solar zenith angle > 90°) or at least analyze the day and night scenes separately.

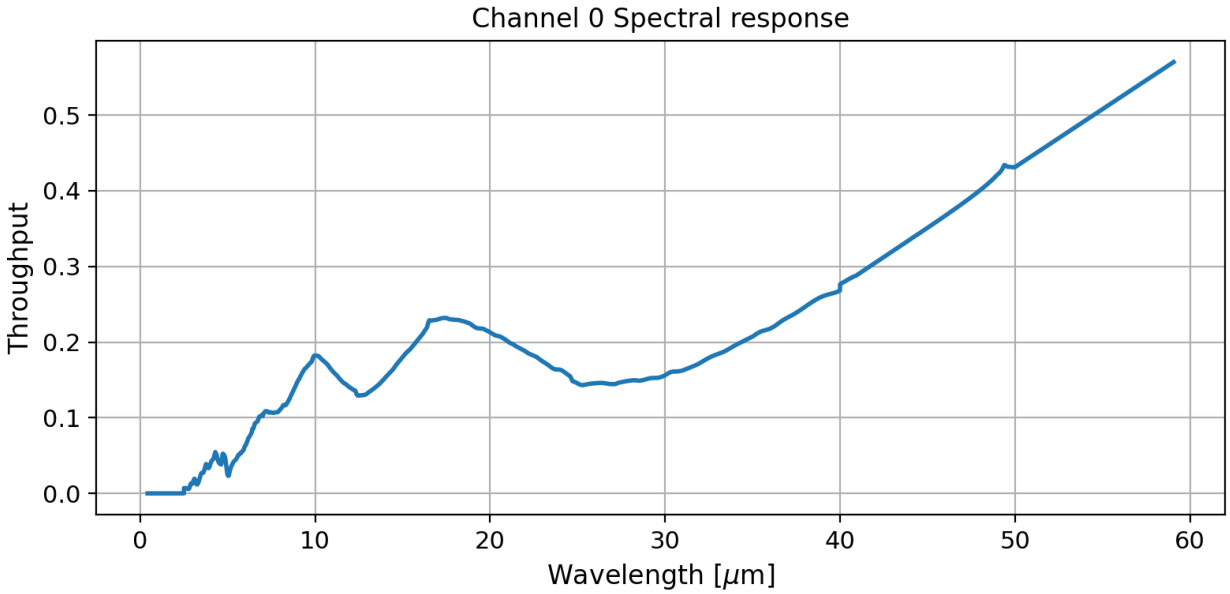

Figure 1-2. The spectral response for the undispersed Channel 0. The response is identical for each PREFIRE-TIRS instrument.

1.2.2 Spatial characteristics

The PREFIRE-TIRS instruments collect data continuously in a pushbroom mode, with an integration time of 0.7 seconds for each data frame. Each data frame contains a spectral measurement from each cross-track scene collected simultaneously. Within this continuous data collection, there are planned interruptions due to calibration cycles or data downlinks, and there are also occasional interruptions due to unplanned instrument operations changes or outages. Each calibration cycle takes ~18.7 seconds for PREFIRE-TIRS1 and ~9.7 seconds for PREFIRE-TIRS2, which implies a gap of approximately 27 and 14 data frames, respectively. Data downlinks create data gaps of up to 13 minutes, and the exact length varies.

Within the orbital swath there are eight distinct tracks of data associated with the eight separate spatial scenes for each PREFIRE-TIRS. The approximate scene footprint sizes are 11.8 km × 34.8 km (cross-track × along-track), with gaps between each scene of approximately 24.2 km. The swath itself is ~264 km across. Note that the scene footprint and swath sizes quoted here are for the orbit altitude soon after launch. However, the footprint size will slowly become smaller as the orbit altitude decreases with time. Do not assume constant footprint or swath dimensions.

PREFIRE-TIRS spatial footprints overlap each other in the along-track dimension. Assuming that no data are missing, any given point along the orbit swath will be observed by up to about 7 overlapping footprints in the along-track direction. The number of footprints that overlap a given footprint will slowly become smaller during the mission, as the satellites' orbital altitudes decrease. Do not assume an integer number of overlapping footprints.

A single data file or granule consists of data collected during approximately one orbit, beginning and ending near the equator to avoid granule borders over the polar regions. Data files are NetCDF4 format and approximately 20-30 MB in size. These data collections are archived at the ASDC DAAC and can

be found at https://asdc.larc.nasa.gov/project/PREFIRE/PREFIRE_SAT1_1B-RAD_R00 and https://asdc.larc.nasa.gov/project/PREFIRE/PREFIRE_SAT2_1B-RAD_R00.

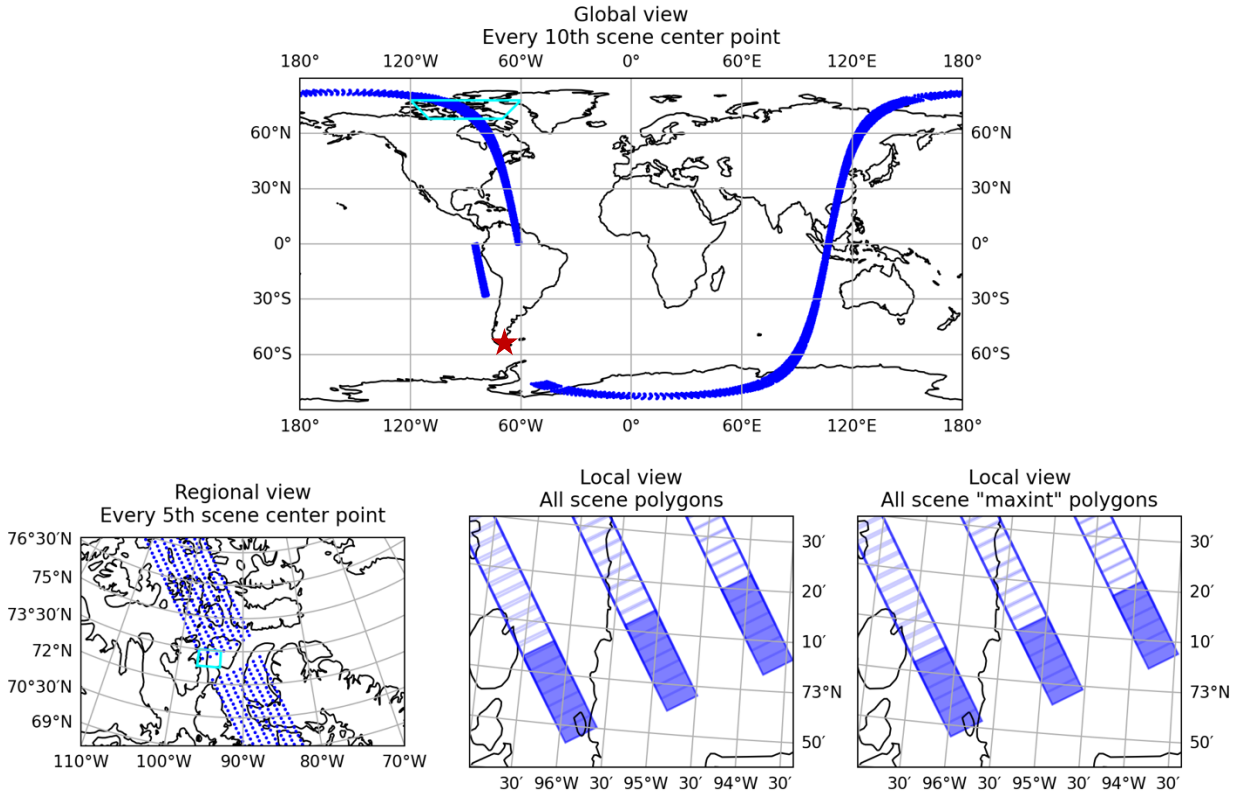

Figure 1-3 shows an example geolocated orbit (top panel) and focused regional and local plots (bottom panels). The global plot was selected to illustrate a data gap due to a data downlink at the Punta Arenas, Chile ground station, from approximately -70°S to -30°S on the ascending pass at the end of the granule. The zoomed in regional view (lower left) shows the data within the small cyan box in the global plot, and illustrates a smaller data gap due to instrument calibration. The local views (lower middle and right) show the actual scene ground footprint polygons, for the cyan box denoted in the regional view. The first scene's polygon is filled blue, to illustrate the shape of the full field of view (FOV) for one data integration. During the 0.7 second integration time, the satellite moves along track slightly more than 5 km, which means the leading and trailing edges of the instantaneous FOV have translated forward by the same amount. The lower right plot shows the "max integration" footprint polygon, which includes the interior portion of the scene footprint that was within the sensor field of view for the entire integration period.

1.3 Purpose

The PREFIRE Level 1B Radiance data product contains the measurement data from each PREFIRE-TIRS instrument in a calibrated, geolocated form that is suitable for further geophysical data product extractions.

2 Product Description

Level 1B Radiance data are calibrated and geolocated radiances. The input data for these collections are also available at the ASDC DAAC. They are as follows:

1. Curated Level 0 Radiance data (collections PREFIRE_SAT1_0-PAYLOAD-TLM and

PREFIRE_SAT2_0-PAYLOAD-TLM)
2. Level 0 spacecraft bus telemetry and engineering data (collections PREFIRE_SAT1_0-BUS-TLM and PREFIRE_SAT2_0-BUS-TLM)

2.1 Algorithm description

The Level 1 data processing algorithm is split into two parts (see Figure 2-4), with the Level 1A portion accomplishing the radiance calibration based on PREFIRE-TIRS telemetry and the Level 1B portion addressing geolocation through the use of spacecraft (bus) telemetry and orbit element sets from satellite ranging observations. In the Level 1A part, the periodic calibration data from each granule are extracted from the datastream and used to form an interpolated instrument thermal profile that enables removal of the instrument thermal background from the Earth observation data. In the Level 1B portion, the timestamps of each frame of calibrated radiance data are correlated with spacecraft location/pointing data and the instrument optical properties are used to determine the ground footprint of each spatial scene.

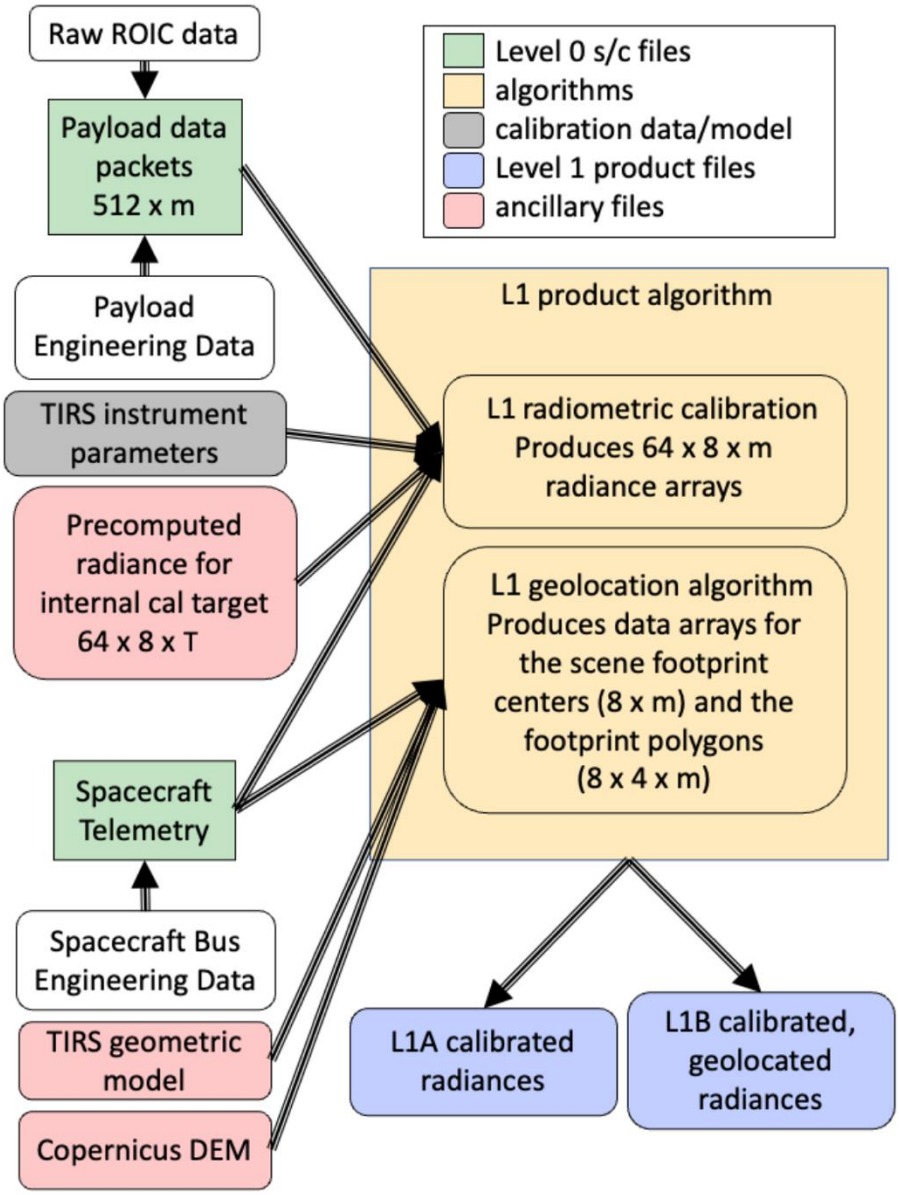

Figure 2-4. Flowchart depicting the input and output data files involved in producing Level 1 (L1) data products. The focal plane array dimensions are given, with the number of along-track frames (*m*), number of pre-computed calibration target temperatures (*T*), and the 4 vertices of the representative footprint polygons indicated.

2.2 File Specifications

2.2.1 File naming convention

File names for this collection follow the following convention:

PREFIRE_SAT<*satID*>_<*productID*>_<*collectionVersion*>_<*internalProductVersion*> <*YYYYMMDDhhmmss*>_<*granuleID*>.nc

For example, a representative Level 1B Radiance product granule collected by PREFIRE-SAT1 on June 1, 2024 would have the following filename:

PREFIRE_SAT1_1B-RAD_R01_P00_20240601185321_00123.nc

2.2.2 File format

PREFIRE 1B-RAD data product files are created in NetCDF4 format with standard metadata. These files can be read with standard NetCDF libraries available in all popular scripting languages and many data visualization programs.

2.2.3 Quality flag and bitflags conventions

The quality of the radiance calibration is affected by many different factors. Users who only need a simple summary of the calibration quality can consult the **_quality_flag* variables containing three states: 0 for "good quality" data, 1 for "uncategorized quality", and 2 for "bad quality" data.

The single summary quality flag that combines all quality information for the *Radiance* data group is *radiance_quality_flag*, which has a three-dimensional (3D) shape that matches the shape of the 3D spectral radiance array (along-track, cross-track, and spectral). Any array elements with a flag value of 2 will have *Fill_Value* in the NetCDF4 variable. Other quality flags (*observation_quality_flag*, *detector_quality_flag*, and *calibration_quality_flag*) can be examined to understand the impact of different aspects of the data context. For example, *observation_quality_flag* gives information about which data frames have bad calibration due to factors that are a function of time and tend to affect all scenes equally.

The *BT* data group has a summary quality flag (*BT_quality_flag*) which should not be assumed to be exactly the same as *radiance_quality_flag*. As these are derived from the *spectral_radiance* values in the *Radiance* data group, the bitflags and secondary quality flags defined there otherwise apply.

The *Channel_0* data group has a summary quality flag (*channel_0_radiance_quality_flag*) and other group-specific quality flags and bitflags. These should not be assumed to be exactly correlated with those in the *Radiance* data group.

In order to fully understand the conditions corresponding to a certain flag, users can consult the associated bitflags arrays contained in the 1B-RAD product granules. These bitflags code for multiple conditions (see Tables 2-6 through 2-8). There is one bitflags array associated with each of the three quality flags (i.e., *observation_bitflags*, *detector_bitflags*, and *calibration_bitflags*). There is no bitflags field associated with *radiance_quality_flag* since that is a combination of all other flagging information into

one array.

2.2.4 Variables

The variable specifications for this collection are described below, with one table devoted to each top-level data group in the NetCDF4 file: *Geometry*, *Radiance*, *BT*, and *Channel_0*. Note that the 1B-RAD *Geometry* group, including all variables, is propagated to every downstream Level 2 data product.

2.2.5 Variable dimensions

A summary of all array dimensions is given in Table 2-1. The *xtrack* dimension is equal to the number of cross-track scenes (8, for both instruments), the *spectral* dimension is equal to the number of spectral channels (63 for both instruments), and the *atrack* dimension is equal to the number of along-track Earth observation data frames in the product. The number of along-track frames varies from orbit to orbit, depending on the timing of downlink contacts, calibration data, and other rarer events. Generally, the maximum is around 7700–7900 frames in one product file, with substantially fewer in granules containing downlinks or unplanned instrument/spacecraft events.

Table 2--1

Dimension	**Abbreviation**
Along-track	*atrack*
Cross-track	*xtrack*
UTC parts	*UTC_parts* (= 7)
FOV (footprint) vertices	*FOV_vertices* (= 4)
spectral channels	spectral
Dimension label	**Definition (C-order)**
1D	(*atrack*)
1Dx	(*xtrack*)
2D	(*atrack*, *xtrack*)
2Dp	(*atrack*, *spectral*)
2Du	(*atrack*, *UTC_parts*)
3D	(*atrack*, *xtrack*, *spectral*)
3Dv	(*atrack*, *xtrack*, *FOV_vertices*)

2.2.5.1 *Geometry* group

The *Geometry* data group consists of all timing, observation geometry, and geolocation variables produced during Level 1B processing (see Table 2-2). This data group and its contents will be replicated within any relevant downstream product (e.g., Level 2 data products), rather than stored as a separate geometry file.

Users of NetCDF software packages that try to automatically decode times should be aware that

these packages may incorrectly interpret the *ctime* variable as a UTC time. The *ctime* variable is a count of total fractional SI seconds since the epoch 2000-01-01T00:00:00 UTC (i.e., no leap second adjustments since that epoch), while the UTC time standard is adjusted to account for all leap seconds. For example, when the PREFIRE *Geometry* group is read by the open_dataset function of the Python xarray package using the default decode_times=True argument, the resulting *ctime* values (with datetime64 data type) will differ from the *time_UTC_values* variable by the number of leap seconds that occurred between 2000-01-01T00:00:00 UTC and the observation time. Users of xarray and other packages that exhibit this behavior are recommended to use *ctime* along with *ctime_minus_UTC* to calculate UTC times if desired, and/or consult *time_UTC_values* to verify the correct UTC timestamps of PREFIRE observations. For example, for an xarray dataset, a datetime64 DataArray could be computed as follows:

```
import xarray as xr
ds = xr.open_dataset({path_to_L1B_product}, group = "Geometry")
ds['UTC_dt64'] = ds['ctime'] – ds['ctime_minus_UTC']
```

Further details on the handling of leap seconds in the CF NetCDF Metadata Conventions can be found in Section 4.4.1 of the CF-1.9 Conventions: https://cfconventions.org/Data/cf-conventions/cf-conventions-1.9/cf-conventions.html#calendar.

Table 2--2

Variable Name	**Type**	**Dimen-sion**	**Units**	**Description**
obs_ID	int64	2D		unique integer identifier for each TIRS look YYYYMMDDhhmmsstbd, composed of UTC date (YYYYMMDD) and time (hhmmss) at TIRS image integration midpoint, t = tenths of seconds [0–9], b = satellite number [1–2], d = scene number [1–8]
ctime	float64	1D	seconds	continuous time since the epoch 2000-01-01T00:00:00 UTC (i.e., similar to TAI) at the midpoint of each TIRS image integration
ctime_minus_UTC	int8	1D	seconds	continuous time minus UTC (i.e., leap seconds since the ctime epoch) at the midpoint of each TIRS image integration
time_UTC_values	int16	2Du	various	UTC datetime at the midpoint of each TIRS image integration, represented as an integer array.

				Array parts: year, month, day, hour, minute, second, millisecond
latitude	float32	2D	degrees_north	topography-corrected latitude of FOV centroid
longitude	float32	2D	degrees_east	topography-corrected longitude of FOV centroid
vertex_latitude	float32	3Dv	degrees_north	topography-corrected latitude for each of the four vertices/corners (arranged counter-clockwise starting at the trailing-left corner) of a 4-sided polygon that closely approximates the geolocated FOV (orbital motion taken into account)
vertex_longitude	float32	3Dv	degrees_east	topography-corrected longitude for each of the four vertices/corners (arranged counter-clockwise starting at the trailing-left corner) of a 4-sided polygon that closely approximates the geolocated FOV (orbital motion taken into account)
land_fraction	float32	2D		land_area / total_area (remainder is water_area) within the FOV, according to the Digital Elevation Model (DEM)
elevation	float32	2D	m	mean topographic elevation within the FOV
elevation_stdev	float32	2D	m	standard deviation of topographic elevation within the FOV
viewing_zenith_angle	float32	2D	degrees	viewing zenith angle at the FOV centroid
viewing_azimuth_angle	float32	2D	degrees	viewing azimuth angle at the FOV centroid (zero is north, clockwise-positive looking down from the zenith)
solar_zenith_angle	float32	2D	degrees	solar zenith angle at the FOV centroid
solar_azimuth_angle	float32	2D	degrees	solar azimuth angle at the FOV centroid (zero is north, clockwise-positive looking down from the zenith)
solar_distance	float64	2D	km	distance from FOV centroid to the solar barycenter
subsat_latitude	float32	1D	degrees_north	sub-satellite latitude
subsat_longitude	float32	1D	degrees_east	sub-satellite longitude
sat_altitude	float32	1D	km	satellite altitude above the geoid at the middle of the xtrack swath
sat_solar_illumination_flag	int8	1D		flag specifying whether the spacecraft is illuminated by the sun; 0=no, 1=partial, 2=full
geoloc_quality_bitflags	uint16	2D		integer composed of bit flags that contain info about the quality of the overall geolocation of each along-track frame of scenes
maxintgz_verts_lat	float32	3Dv		latitude (topographically-corrected) for

				each of the four vertices/corners (arranged counter-clockwise starting at the trailing-left corner) of a 4-sided polygon that closely approximates the geolocated zone with the maximum TIRS image integration time
maxintgz_verts_lon	float32	3Dv		longitude (topographically-corrected) for each of the four vertices/corners (arranged counter-clockwise starting at the trailing-left corner) of a 4-sided polygon that closely approximates the geolocated zone with the maximum TIRS image integration time
orbit_phase_metric	float32	1D	degrees	orbit phase angular metric (range of 0-360 degrees, varying approximately linearly with time), defined as 0 deg at the ascending node (northward equator crossing) of the satellite orbit, 180 deg at the descending node, and so on
satellite_pass_type	int8	1D		flag specifying which type of satellite pass each frame is mostly/all part of. −1 = descending, 1 = ascending

2.2.5.2 *Radiance* group (calibrated, geolocated, spectral radiance)

The specifications for the calibrated and geolocated spectral radiance field and associated uncertainties, quality flags, and bitflags are provided in Table 2-3.

Table 2--3

Variable Name	Type	Dimen-sion	Units	Description
detector_ID	int16	2Dp		unique integer identifier for each TIRS detector, cNN, composed of c = scene number [1–8], NN = channel number [0–63]
detector_bitflags	uint16	2Dp		integer composed of bit flags that contain info about each TIRS channel/scene combination, for this granule
wavelength	float32	2Dp	μm	center wavelength of each spectral channel, given by the SRF-weighted mean over wavelength
idealized_wavelength	float32	2Dp	μm	center wavelength of each spectral channel, in the idealized spectrometer grid
spectral_radiance	float32	3D	W/(sr m^2 μm)	spectral radiance
spectral_radiance_unc	float32	3D	W/(sr m^2 μm)	uncertainty of spectral radiance
observation_bitflags	uint16	1D		

calibration_bitflags	uint8	3D		
observation_quality_flag	int8	1D		Specifies the quality of the data frame. Main purpose is to flag time periods (e.g., eclipse entrance, instrument temperature out of range, …) with data quality issues
radiance_quality_flag	int8	3D		**The primary, combined quality flag**, which merges information from the different quality flags. Understanding why certain values were flagged as bad requires examining other quality_flag and/or bitflag arrays.
calibration_quality_flag	int8	3D		Full 3D array to capture problems in the L1A calibration calculation, which can happen at certain times for certain scene+channel combinations
detector_quality_flag	int8	2Dp		Specifies the quality of the detector elements. This array flags conditions of the physical FPA detector elements, e.g., "noisy" or "dead pixels"

2.2.5.3 *BT* group (calibrated, geolocated, spectral brightness temperature)

The *BT* data group contains similar data (see Table 2-4) to the *Radiance* group, with most radiances converted to brightness temperatures.

Table 2--4

Variable Name	Type	Dimension	Units	Description
spectral_BT	float32	3D	K	spectral brightness temperature
spectral_BT_unc	float32	3D	K	uncertainty of spectral brightness temperature
BT_quality_flag	int8	3D		quality flag for spectral_BT

2.2.5.4 *Channel_0* group (calibrated, geolocated radiance)

The *Channel_0* data group contains radiance for channel 0, which is illuminated by undispersed light (see Table 2-5). Thus, the radiance for channel 0 is not spectral, and it is related to the total broadband radiation in the observed scene.

Table 2--5

Variable Name	Type	Dimen-	Units	Description

		sion		
channel_0_radiance	float32	2D	W/(m^2 sr)	total spectrally integrated radiance from direct-illuminated TIRS channel 0
channel_0_radiance_unc	float32	2D	W/(m^2 sr)	channel 0 radiance uncertainty
channel_0_detector_ bitflags	uint16	1Dx		integer composed of bit flags that contain boolean info about TIRS channel 0 for each scene
channel_0_detector_ quality_flag	int8	1Dx		quality flag describing characteristics of channel 0 detectors
channel_0_radiance_ quality_flag	int8	2D		overall spectral radiance quality flag, representing the combination of any detector, observation, and radiance quality flags for channel 0

2.2.6 Bitflags definitions

For each bit-flagged condition listed in the tables below, the third column lists the Quality Flag (QF) value associated with that condition. A QF value of 2 means that any of the associated data values will have a QF value of 2 if that condition is met. When the different flags are merged in the summary quality flag (e.g., *radiance_quality_flag* for the *Radiance* data group), values of 2 will take precedence. For example, if *observation_quality_flag* is 2 for frame 1234 in a particular granule, all spectral channels in all scenes for that data frame will have *radiance_quality_flag* of 2, regardless of the *detector_quality_flag* and *calibration_quality_flag* values for that data frame.

2.2.6.1 Detector bitflags

Masked detectors and extreme-noise or unresponsive detectors are the only conditions that are mapped to QF 2 (bad quality). The masked channels are 1, 2, 3, 8, 9, 17, 18, 35, and 36. The remaining conditions identify detectors with potential quality issues, but for which the quantitative impact has not been fully assessed. Analyses performed with these channels should be done with caution. This is relevant for both *detector_bitflags* (*Radiance* data group) and *channel_0_detector_bitflags* (*Channel_0* data group).

Figure 4-1 shows the quality flag as a two-dimensional image (spectral x cross-track scene). Bit 3 is currently set in the shorter wavelength channels (channels 4, 5). Bit 4 is set for the longest wavelength band (FIR-2; channels 37–63). Finally, bit 5 is set for the two channels near the masked channel gap between the MIR-2 and FIR-1 bands (channels 19 and 20 for PREFIRE-TIRS1, and channels 16 and 19 for PREFIRE-TIRS2).

Table 2--6

Bit	Meaning	QF value
0	Detector masked	2
1	Extreme noise or unresponsive detector	2
2	Greater-noise category	1
3	Unreliable calibration due to stray light contribution	1
4	Unreliable calibration due to thermal effects	1
5	Unreliable calibration due to filter-edge effects	1

6–15	Unused	

2.2.6.2 Calibration bitflags

Calibration bitflags denote cases where the calibration failed due to numerical errors, or if the calibration was not attempted. The latter is true for only the masked channels.

Table 2--7

Bit	Meaning	QF value
0	Invalid calibration	2
1	Calibration not attempted (masked detector)	2
2–7	Unused	

2.2.6.3 Observation bitflags

The observation bitflags describe various conditions that are generally related to the condition of the spacecraft or instrument. These conditions are a function of time and will apply equivalently to all scenes and detectors.

Table 2--8

Bit	Meaning	QF value
0	Thermal transient after payload-on-but-safed period (e.g., during/near downlink contacts and GPS zenith pointing)	1
1	Small thermal/radiometric perturbation present (e.g., near eclipse exit)	1
2	Large thermal/radiometric perturbation present (e.g., near eclipse entrance)	2
3	Greater-than-normal temperature change within this orbit (during the thermal transient after powering instrument back on)	1
4	Moderate time interval between observation and the nearest calibration sequence (due to corrupted or missing calibration sequence(s))	1
5	Large time interval between observation and the nearest calibration sequence (due to corrupted or missing calibration sequence(s))	2
6	Bus telemetry indicates that spacecraft attitude determination is invalid	2
7	Lack of spacecraft attitude information due to a bus telemetry gap	1
8	During an unknown type of bus slew	1
9	During a modeled-sun-avoidance type of bus slew	2
10	Electronics warm-up period after powering instrument on	2
11–15	Unused	

3 Updates Since the Previous Data Product Version (R00)

- Filenames were modified in order to make data searches more efficient
  - was: PREFIRE_*_P00_R00_*.nc
  - now: PREFIRE_*_R01_P00_*.nc
- PREFIRE-SAT2 geolocation was systematically shifted “uptrack” by about 10 km, in order to center the observed geolocation uncertainty distribution around zero

- Fixed incorrect *geoloc_quality_bitflags* (*Geometry* data group) values
- Upstream changes to 1A-RAD processing (see *PREFIRE Data User Guide for 1A-RAD Version R01*). A relatively small number of PREFIRE-SAT1 1B-RAD granules should contain more-accurate radiances and/or geolocation due to one of these changes.
- In order to reduce the necessary storage and data transfer bandwidth, some supporting variables' precision was appropriately reduced
    - in the *Geometry* data group: *latitude, longitude, vertex_latitude, vertex_longitude, elevation_stdev, subsat_latitude, subsat_longitude, maxintgz_verts_lat, maxintgz_verts_lon, elevation, viewing_zenith_angle, viewing_azimuth_angle, solar_zenith_angle, solar_azimuth_angle, orbit_phase_metric*
    - in the *Radiance* data group*: wavelength, idealized_wavelength*
- Radiance and BT uncertainties are now set to *Fill_Value* when the associated radiance/BT is *Fill_Value*
- Aesthetic changes were made to some *Fill_Value* usage and variable attribute datatypes
- An improved categorization algorithm for PREFIRE-SAT1 payload data frames is now being operationally used, greatly reducing the number of missed calibration sequences and misclassifications of data frames (e.g., non-Earth-view data erroneously treated as Earth-view data).

4 Known Issues

PREFIRE-SAT1 only:

For TIRS2 nearly all payload data frames can be properly categorized (as Earth-view, space-view, calibration target, etc.) using the mirror motor encoder position information alone. In contrast, before launch, robust mirror motor encoder position information from TIRS1 (PREFIRE-SAT1) was permanently lost. Nevertheless, after launch the PREFIRE team was able to modify the science mode operation strategy for the TIRS1 mirror motor to obtain information crucial to both radiance calibration and geolocation. A payload data frame categorization algorithm for TIRS1 was developed that uses payload engineering temperatures, bus telemetry, and the spectroradiometer DNs (counts) themselves. However, due to the real-world complexity and shortcomings of the input data streams, the algorithm can occasionally miss calibration sequences, misclassify non-Earth-view data as Earth-view data (and vice versa), and even more rarely degrade geolocation accuracy. These occurrences account for only a small fraction of the PREFIRE-SAT1 dataset, however, and will be further reduced in subsequent data releases (as on-orbit experience is gained, and the algorithm is improved).

Geolocation:

The GPS receiver on PREFIRE-SAT1 has performed poorly since launch, and the GPS receiver on PREFIRE-SAT2 ceased to function well at the end of August 2024. Because of the lack of continuously reliable GPS position and time data, the time-dependent orbital position and velocity vectors used for geolocation are based on orbital reconstructions. This uses publicly available orbit element sets (e.g., Two-Line Element sets (TLEs) based on ranging observations by the United States Space Force and other entities. The precision and accuracy of the orbit reconstruction is currently undergoing evaluation. In addition, residual uncertainties exist due to pointing offsets from lack of precise knowledge of the spectrometer slit orientation relative to the

spacecraft. These uncertainties will be addressed after the orbit reconstruction is evaluated and optimized. The current best estimate is that individual geolocated scenes could have along-track geolocation errors of up to 50 km with an average uncertainty of approximately 30 km (less than the along-track dimension of a ground footprint). The cross-track geolocation error has not been quantified, but the error is likely to be less than the cross-track scene width (approximately 12 km), based on favorable spatial correlations with co-located geostationary imagery collected in the MIR atmospheric window.

As more PREFIRE-TIRS data are collected and analyzed, the quantification of the geolocation uncertainties will improve. Further refinements of the geolocation algorithm are planned, which will reduce these errors in future 1B-RAD data product releases.

Detector status:

A small number of detectors in each instrument FPA are non-responsive. Some of these are due to the instrument design (masked pixels at the order-sorting filter edges) and some are due to individual detector failures. These are marked within the detector bitflags (see section 2.2.6.1). Figure 4-1 shows the distribution of these pixels across each instrument FPA. No new unresponsive detector elements have been noted in flight data, relative to the known list of unresponsive detector elements identified from analysis of pre-launch test data.

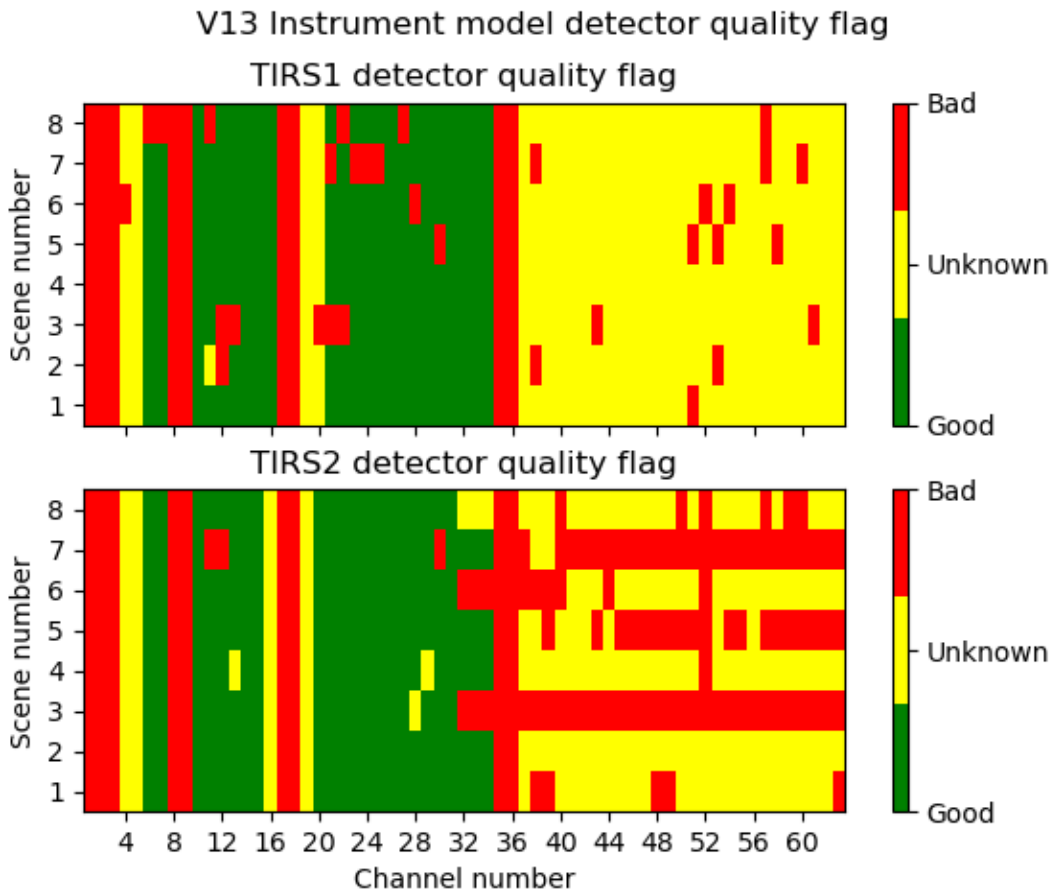

Figure 4-1: Two-dimensional maps of the detector quality flag from each PREFIRE-TIRS. The vertical red bars ("bad" quality) are the locations of the masked pixels. The remaining red elements are the locations of extreme-noise or non-responsive elements.

Radiometric calibration:

Overall, the data from the MIR-2 and FIR-1 bands have the highest calibration quality (green channels in Figure 4-1). Channels in other filter blocks are subject to various calibration issues, as described below.

Stray light in shortwave channels.
The shorter-wavelength channels (λ ~3–5 μm, channels 4–5) in MIR-1 appear to have stray light or out-of-band contributions that are not characterized. The effect is strongest at the shortest wavelength channels, and these show large biases when compared to independent radiance estimates, such as forward-modeled radiance from meteorological reanalysis data. This effect is captured by the detector bitflags (see Table 2-6), and these channels are marked as "uncategorized" calibration quality.

Calibration errors at band edges.
Channels near the band edges adjacent to the CO_2 absorption band at ~15 μm show increased bias relative to independent radiance estimates (forward-modeled radiance or co-locations with other infrared spectrometers). These channels are marked with the detector bitflags (see Table 2-6) and are marked as "uncategorized" calibration quality.

Unreliable background and gain estimation of FIR-2 channels.
The current radiometric calibration method is not performing well for the longest wavelength channels. Due to thermal drifts of the order-sorting filter for FIR-2, and low signal levels (particularly for the longest wavelengths), the calibrated radiance shows large bias errors relative to forward-modeled radiance. Planned improvements to the calibration algorithm will improve these channels in future data releases. Currently these are marked in the detector bitflags (see Table 2-6) and marked as "uncategorized" calibration quality.

Electronic pattern noise.
Electrical cross talk between adjacent FPA detectors was largely mitigated by alternating the wiring polarity in the readout integrated circuits. However, residual pattern noise has been noted in both the raw data and the calibrated radiances. This noise is highly temporally correlated and impacts all spectral channels.

This electrical noise manifests in two primary ways. First, "sawtooth-like" patterns can be visible in an individual spectral observation, where the even and odd spectral channels have different radiometric biases. These patterns are generally visible in spectral residuals (observation – modeled radiance). Due to the temporal correlation this pattern could be visible in multiple consecutive frames. Second, "striping" is visible when data from a selected channel are viewed spatially, where specific spatial scenes are clearly biased relative to the other scenes. Again, due to the temporal correlation these stripes will continue along track for some time. No data flagging is performed related to this pattern noise effect, but future developments in the calibration algorithm are planned to further reduce this noise.

Eclipse transition features.
Close to when the satellite passes into or out of eclipse (where the satellite is within Earth's shadow from the sun), it is thought that solar radiation briefly impinges at a large oblique angle on an instrument casing (eclipse entrance) or on the onboard calibration target (eclipse exit). The subsequent out-of-family heating and thermal emission manifest as transient signals within the instrument data time series, which cannot be correctly modeled with the current calibration scheme. These data are flagged (see Table 2-8). In current operations the eclipse entrance data have far larger calibration errors which can be identified through assessments of relative calibration. In other words, analysis of the eclipse entrance data shows that it is inconsistent with other data collected by PREFIRE-TIRS. The eclipse exit features typically show less impact on the relative calibration, but the impact on the absolute calibration is not currently understood. Initial analysis shows that the absolute calibration (as assessed by comparison to independent radiometric data) may change during the eclipse exit transitions. The current strategy is to flag data collected during eclipse entrances as bad and remove them from the 1B-RAD data product, and to flag data collected during eclipse exits as "uncategorized quality", to caution users that there may be unquantified biases.

Due to the changing sun-satellite geometry throughout Earth's orbit, the relative timing and location of the eclipse features have seasonal variation. Furthermore, since the solar angles during eclipse transitions also change with season, the quantitative impact of these features may change throughout the mission. Figure 4-2 shows the geolocated scene footprints from an example granule (approximately an orbit), where different data quality states are visualized.

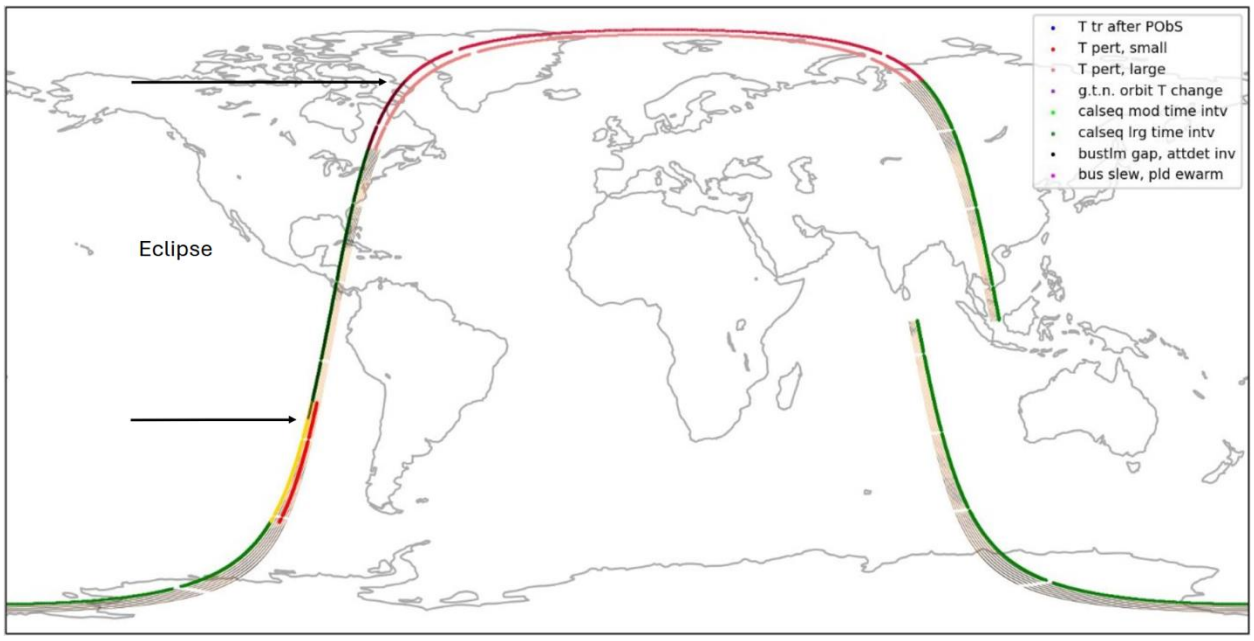

Figure 4-2: Sample visualization of a PREFIRE 1B-RAD granule, with data quality conditions (vivid colors) overlaid on radiance in channel 14 (muted tones) plotted along the orbit track. Note that each condition described affects all 8 cross-track scenes equally. Different colors are overplotted on single scenes to allow for multiple conditions to be visually displayed in the figure. The upper (northmost) scene in the track encodes the final quality flag (*radiance_quality_flag*) status of the data, marked with red, yellow, or green, similarly to figure 4-1. The occasional lower colored band corresponds to the legend and

shows *observation_bitflags* values of interest. Of note is the eclipse entrance feature, over much of the Arctic, and the eclipse exit feature west of South America.

5 Resources

The Algorithm Theoretical Basis Document (ATBD) can be found at https://prefire.ssec.wisc.edu/Documents/PREFIRE_1A-RAD_1B-RAD_ATBD.pdf. For more information, contact Erin Hokanson Wagner at prefire-sdps.admin@office365.wisc.edu.

6 References

L'Ecuyer, T.S., Drouin, B.J., Anheuser, J., Grames M., Henderson, D., Huang, X., Kahn, B.H., Kay, J.E., Lim, B.H., Mateling, M., Merrelli, A., Miller, N.B., Padmanabhan, S., Peterson, C., Schlegel, N.-J., White, M.L., Xie, Y., "The Polar Radiant Energy in the Far-InfraRed Experiment: A New Perspective on Polar longwave Energy Exchanges," *Bulletin of the American Meteorological Society (BAMS*), 102(7), E1431–E1449, 2021.

Padmanabhan, S., Drouin, B., L'Ecuyer T., White, M., Lim. B., Kenyon, M., Mariani, G., McGuire J., Raouf, N., De Santos, O., Bendig, R., "The Polar Radiant Energy in the Far-InfraRed Experiment (PREFIRE)," *IGARSS 2019 – 2019 IEEE International Geoscience and Remote Sensing Symposium*

Citation

DOI:

- PREFIRE_SAT2_1B-RAD_R01: 10.5067/PREFIRE-SAT2/PREFIRE/RAD_L1B.R01
- PREFIRE_SAT1_1B-RAD_R01: 10.5067/PREFIRE-SAT1/PREFIRE/RAD_L1B.R01

7 Appendix

Table 7-1 shows the channel wavelengths for both PREFIRE-TIRS instruments. Both the idealized central wavelengths and the mean (SRF-weighted) wavelengths are listed, all in units of micrometers.

Table 7--1

	PREFIRE TIRS1		PREFIRE TIRS2			PREFIRE TIRS1		PREFIRE TIRS2	
Ch #	Ideal λ	Mean λ	Ideal λ	Mean λ	Ch #	Ideal λ	Mean λ	Ideal λ	Mean λ
1	masked				35	masked			
2	masked				36	masked			
3	masked				37	30.80	31.16	32.05	32.17
4	2.95	3.92	4.20	4.47	38	31.64	31.84	32.89	32.92
5	3.80	4.26	5.05	5.10	39	32.49	32.55	33.74	33.78
6	4.64	4.76	5.89	5.89	40	33.33	33.36	34.58	34.67
7	5.48	5.51	6.73	6.31	41	34.17	34.23	35.42	35.49
8	masked				42	35.02	35.09	36.27	36.28
9	masked				43	35.86	35.91	37.11	37.09
10	8.02	8.40	9.27	9.29	44	36.71	36.68	37.96	37.93
11	8.86	8.90	10.11	10.16	45	37.55	37.51	38.80	38.80
12	9.70	9.76	10.95	10.98	46	38.39	38.39	39.64	39.67
13	10.55	10.59	11.80	11.80	47	39.24	39.25	40.49	40.53
14	11.39	11.41	12.64	12.62	48	40.08	40.12	41.33	41.35
15	12.24	12.23	13.48	13.38	49	40.92	40.93	42.17	42.17
16	13.08	13.04	14.33	13.87	50	41.77	41.81	43.02	42.99
17	masked				51	42.61	42.55	43.86	43.83
18	masked				52	43.46	43.47	44.71	44.65
19	15.61	15.96	16.86	16.89	53	44.30	44.19	45.55	45.56
20	16.45	16.51	17.70	17.74	54	45.14	45.19	46.39	46.33
21	17.30	17.33	18.55	18.59	55	45.99	45.88	47.24	47.34
22	18.14	18.18	19.39	19.43	56	46.83	46.94	48.08	47.97
23	18.99	19.02	20.24	20.28	57	47.68	47.61	48.92	49.10
24	19.83	19.86	21.08	21.11	58	48.52	48.57	49.77	49.70
25	20.67	20.71	21.92	21.96	59	49.36	49.43	50.61	50.59
26	21.52	21.54	22.77	22.79	60	50.21	50.09	51.46	51.51
27	22.36	22.39	23.61	23.62	61	51.05	51.12	52.30	52.26
28	23.20	23.22	24.45	24.46	62	51.89	51.90	53.14	53.09
29	24.05	24.05	25.30	25.29	63	52.74	52.66	53.99	54.11

30	24.89	24.89	26.14	26.11					
31	25.74	25.71	26.99	26.96					
32	26.58	26.54	27.83	27.81					
33	27.42	27.40	28.67	28.62					
34	28.27	28.23	29.52	29.45					